THE USE OF MODELLING TECHNIQUES TO DESCRIBE RECRYSTALLIZED GRAIN SIZE OF COMMERCIALLY PROCESSED 6000 SERIES ALUMINIUM ALLOY COMPONENTS

M.R. Clinch*, S.W. Christensen**, P.A.S. Reed**, I. Sinclair**,
W. Hepples*, and N.J.H. Holroyd***

*Luxfer Gas Cylinders, Nottingham NG4 2BH, England.
**Materials Research Group, School of Engineering Sciences,
University of Southampton, Southampton SO17 1BJ, England.
***Luxfer Gas Cylinders, Riverside, CA 91250 USA.

ABSTRACT

The development of grain size during commercial thermomechanical processing of 6000 series aluminium alloy components has been investigated by combining physical experiments and modelling techniques. A range of grain structures was generated by varying both deformation temperature and heat treatment practice. The different deformation conditions were simulated by finite element modelling, which allowed parameters such as plastic strain, strain rate and deformation temperature to be subsequently extracted. An adaptive numeric technique (neurofuzzy modelling) was employed to describe the recrystallized grain size in terms of the process parameters, and its performance compared with that of an empirical relationship from the literature.

1. INTRODUCTION

The Al-Mg-Si 6000 series alloys are used extensively for wrought products serving a wide range of commercial applications. For example, high pressure gas cylinders are manufactured from AA6061 alloy by a two-stage deformation process, cold backward extrusion followed by warm neck forming [Woodward and Bates (1987)]. Solution and precipitation heat treatments are carried out to achieve the desired balance of strength, toughness and resistance to environmentally sensitive degradation required in the final product. Previous annealing studies by Clinch, Harris, Hepples, Holroyd and Wood (2000) on cold worked material revealed classic Johnson-Mehl-Avrami-Kolmogorov (JMAK) type behaviour, with recrystallization occurring readily at all temperatures investigated. In commercial practice, however, recrystallization takes place whilst heating to the solution heat treatment temperature rather than during an isothermal anneal. The non-homogeneous nature of the deformation processes employed can lead to a range of grain sizes being present within the heat treated component and furthermore, grain

structure has been found to vary with both deformation and heat treatment conditions. Exact processing conditions will not be discussed in this paper due to commercial sensitivity of the information.

Whilst physical understanding of microstructure development may be well developed for specific simplified conditions, accurate quantitative modelling of more complex, multivariate and essentially 'noisy' industrial systems may be efficiently addressed by adaptive numeric modelling methods such as neural networks, neurofuzzy networks and Support Vector Machines [Christensen et al., (2000), Brown and Harris, (1994)]. These are established in predictive modelling in a variety of disciplines (e.g. financial markets analysis, weapons tracking systems, speech recognition) constituting a considerable improvement over simple regression analyses often used in production engineering environments. In the present study neurofuzzy modelling has been applied as an extension to detailed finite element modelling, forming a uniquely integrated modelling/simulation effort.

2. EXPERIMENTAL METHODS

2.1 Materials and techniques. Commercial DC cast AA6061 material was used throughout this study, which had been stress relieved and homogenised to give suitable microstructure and properties for downstream processing [Holroyd and Hepples (1999)]. Billets were extruded at room temperature to a true strain of 1.87, or 85 % reduction in area, to provide samples for hot working trials. A common pre-heat was employed in all cases, but delay time prior to working was varied to give six initial deformation temperatures. All variants were then subjected to a standard solution heat treatment and ageing practice for the alloy. This was carried out in both a commercial oven and a salt bath furnace, giving 'slow' and 'fast' heating rates respectively.

Specimens were prepared for optical microscopy using standard metallographic techniques for aluminium alloys and anodised in Barkers Reagent in order to reveal grain structures. The linear intercept method was used to measure grain size at selected locations within the component.

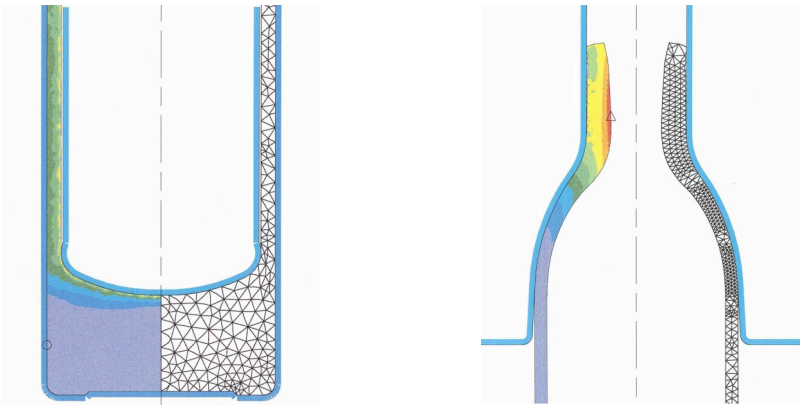

(a) (b)

Figure 1. Examples of finite element model contour maps showing distribution of plastic strain after (a) deformation 1, and (b) deformation 2.

2.3 Finite element modelling. The cold extrusion and subsequent hot forming operation were modelled as separate processes, referred to hereafter as "deformation 1" and "deformation 2" respectively. Initial conditions based on temperature measurements after pre-heating were specified for the six variants prior to deformation 2. Examples of strain contour plots from each deformation process are shown in Figure 1(a) and 1(b) respectively. Process history information

was extracted for specific geometric locations within the final component where grain size had also been measured. These parameters were used as input values for subsequent analysis and adaptive numeric modelling work.

Recrystallized grain size was calculated in terms of the prior deformation parameters according to Equation (1) below, stated by Humphreys and Hatherly (1995), where the coefficients *c, c′, n,* and *k* were obtained via linear regression. Since no expression for heating rate is included, grain size was determined for oven heat treated material only.

$$D_{rex} = cD_0^{c'}\varepsilon^{-n}z^{-k} \quad (1)$$

where *c, c′, n, k* = constants; D_0 = original grain size; ε = plastic strain; z = Zener Holoman parameter (Q = 205 kJ/mol)

2.3 Adaptive Numeric Modelling. The neurofuzzy (NF) modelling approach used in this work is essentially a neural network (NN) incorporating fuzzy logic [Brown and Harris, (1994)]. Where the ordinary NN [Bishop, (1995)] relies on simple functions of all inputs woven into an obscure network, the NF model, during optimisation, adapts its internal structure, identifying only the relevant inputs and their interactions. Model complexity is limited (via a statistical significance term) to a level which is justified by the amount and distribution of data. Models are therefore kept simple, normally relying on subfunctions of less than 4 input parameters and, consequently, are highly transparent, such that relationships between individual input parameters and the output parameter are easily identified.

Final microstructure in the component is determined by both deformation stages and heat treatment conditions. Deformation 1 was represented by plastic strain with a hardness multiplier term to account for annealing prior to deformation 2, which was described by plastic strain, strain rate and temperature. Heat treatment medium was included as a binary input, indicating either "slow" air oven or "fast" salt bath. The full set of inputs was therefore: $Strain_1$, Multiplier, ($Strain_1$*Multiplier), $Strain_2$, $Strain\ rate_2$, $Temperature_2$ and Solutionising Medium. A total of 64 data points were modelled, using both measured grain size values and their natural logarithms. As a benchmark for the NF modelling, linear multivariate regressions (least squares) were carried out and both techniques compared to empirical modelling described by Equation (1).

3. RESULTS AND DISCUSSION

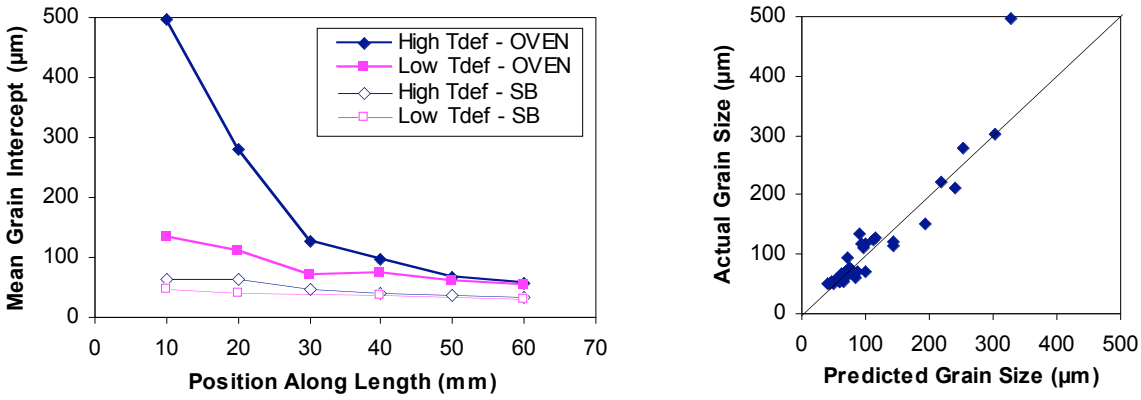

(a) (b)

Figure 2. (a) Effect of deformation temperature and heat treatment medium on grain, and (b) predicted vs. actual grain size according to Equation (1).

Figure 2(a) shows examples of heat treated grain size as a function of position within the component for the highest and lowest of the six deformation temperatures, after both heat treatment conditions, and indicates the range of grain sizes encountered. The largest grain sizes were observed at combinations of high deformation temperature and slow (oven) heating rate, however in all cases grain size appeared to decrease along the length of the component. The apparent grain refinement due to rapid (salt bath) heating was less pronounced in material deformed at low temperature. Figure 2(b) shows performance of the empirical model based on Equation (1) for the oven heat treated data. Whilst in general predicted grain sizes were fairly close to actual values, significant deviation from the empirical model was experienced at the highest point.

Table 1. Linear regression, neurofuzzy and empirical model performance.

Model		Target **	Training		Test	
No	Type*		MSE***	MRE (%)****	MSE***	MRE (%) ****
1	LLS	GS	2768.8	51.3	3516.5	58.3
2	LLS	ln(GS)	2028.6	21.3	2409.5	24.0
3	NF	GS	708.5	14.4	902.4	15.6
4	NF	ln(GS)	824.1	13.4	980.2	14.9
5	EMP	ln(GS)	1071.0	14.3	-	-

* LLS refers to linear least squares regression, NF neurofuzzy, EMP empirical (eqn. 1)

** Models 2,4 and 5 model ln(grain size). In order to compare their MSEs to those of the other models, their outputs were transformed to grain size values and regular MSEs obtained.

*** Grain sizes are in μm, MSEs in μm^2.

**** Values are based on actual rather than logarithmic grain size values in models 2, 4 and 5.

Table 1 shows model performance for the linear regression, NF and empirical methods. Errors are shown in terms of: (i) the mean-squared-error (MSE), based on the absolute errors between model predictions and experimental results, and (ii) the mean relative error (MRE), where the errors between prediction values and experimental results are expressed as percentages of the experimental value. MRE gives a fairer comparison of model performance across the wide range of grain sizes being considered. When reviewing MSE and MRE values it may be noted that 95% confidence limits on the measured grain dimensions were of the order of 9.6%. The training errors were found by establishing the model based on all data points and then calculating the prediction error, i.e. the difference between model prediction and actual output value, for all data points. Given the relative paucity of data, test errors were assessed via leave-one-out cross-validation, whereby multiple modelling is carried out with a different single point left out of the training set each time. This is conducted for all of the data, with modelling error then being expressed in terms of the average error between model prediction and target value for the unseen points.

Overall it may be seen that the NF models provide the best prediction accuracy, with the similarity in training and test errors showing that overfitting had not occurred. It is interesting to note that whilst LLS accuracy improved on using logarithmic data; this was not the case for the NF modelling; a result of its intrinsic functional flexibility, using piecewise functions as necessary. The empirical model showed some improvement over the basic LLS model, particularly in the MRE values, and performance was comparable to those of the NF models, although this is not a fair comparison, as Equation (1) is only applicable to one solution treatment condition.

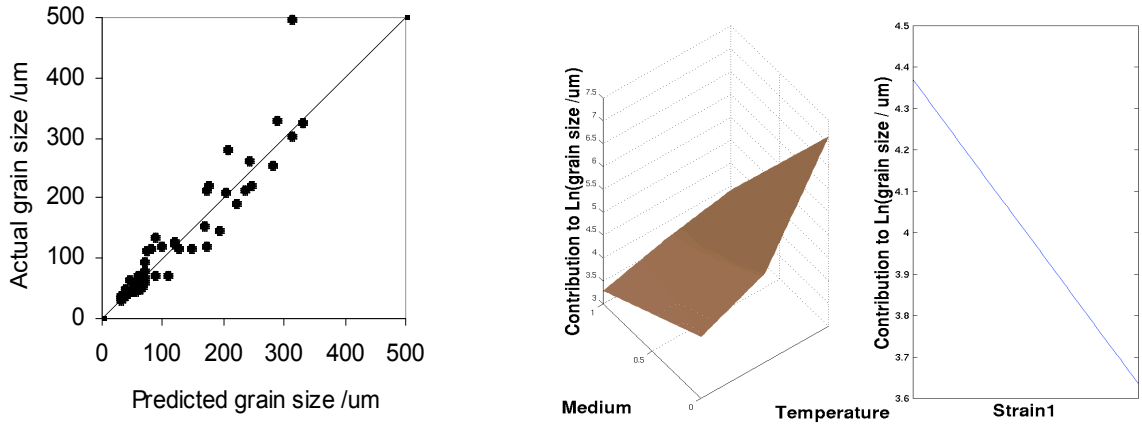

(a) (b)

Figure 3. (a) Model prediction versus experimental values plot for NF model No. 4, and (b) neurofuzzy sub-function plots.

The general quality of model accuracy of the NF-type models across the complete grain size data range is illustrated by the prediction versus experimental values plot shown in Figure 3(a) for model No. 4 in Table 1. NF model 4 (with the best MRE) gave the sub-function structure and corresponding regression surfaces shown in Figure 3 (b). Whilst higher order functions were available to the NF models, only piecewise linear subfunctions were allowed, so as to pre-constrain model complexity in light of the low number of data points. The underlying trends are clearly identified as: (i) increasing grain size after solutionising in the air oven (in Figure 3(b) solutionising medium values of 0 and 1 correspond to the air oven and salt bath respectively), (ii) increasing grain size with $Temperature_2$, and (iii) decreasing grain size with increasing $Strain_1$. The increased sensitivity to temperature in the oven treated condition is clearly evident in the bivariate function. It is interesting to note that whilst the continuous function of solutionising medium 'value' (i.e. going from 0 to 1) is rather artificial; this range may be broadly linked to continuous variations in the solutionising heat rate.

The NF modelling results may be viewed with a degree of confidence in light of qualitative physical understanding of the system and the model structure shown in Figure 3(b) - this highlights the role of model transparency in the modelling process, with such assessment of functionality being highly problematic in conventional NN techniques. Specifically, the solution heat treatment medium should have a distinct effect on recrystallisation, with the rapid salt bath heating rates essentially inhibiting recovery, leading to more stored energy being retained at the onset of recrystallization and hence smaller grain size for a given plastic strain. Furthermore, increasing deformation temperature will effectively reduce the stored energy for a given strain due to dynamic recovery. It is significant to note that the NF modelling actually used a rather limited number of inputs to achieve the predictions. This may be attributed to the input data ranges, as the technique is purely data driven and cannot find relationships where parameters are of an effectively limited range. For example, the range of strain rates during deformation 2 would not be expected to have a strong influence given the temperatures involved, hence the absence of a strain rate term in the NF models is not unreasonable. This is an important fundamental issue with data driven modelling of any degree of sophistication - such techniques may therefore be of considerable value in practical situations, where parameter ranges and correlations are closely defined by the process of interest, but extrapolation of the relationships that are found must be treated with caution. The apparent inability of all models, including the

empirical approach, to predict the large grain sizes observed at combinations of high deformation temperature and oven heat treatment is of particular interest and requires further investigation. It is possible that extensive dynamic recovery may have occurred during deformation, leading to a significant reduction in nucleation sites for recrystallization. In this case final grain size would be controlled by grain growth rather than nucleation, and therefore might be expected to follow Equation (2) below rather than Equation (1) [Humphreys and Hatherly (1995)].

$$D^n = D_{rex}^n + c\ t\ exp\ (-Q_g / kT) \qquad (2)$$

where c, n, Q_g = constants

4. CONCLUDING REMARKS

This study has shown that finite element modelling can provide details of deformation parameters necessary to develop microstructural models for real industrial processes. Furthermore, the application of adaptive numeric modelling approaches offers good prediction accuracy, whilst being more comprehensive than the conventional empirical approach in being able to include heating rate effects.

ACKNOWLEDGEMENTS

This research collaboration was carried out as part of the Luxfer Advanced Technology Centres (ATC) network. One of the authors (M.R. Clinch) also wishes to thank The Royal Commission for the Exhibition of 1851 and Dr T.J. Sabin.

REFERENCES

Bishop, C.M., (1995), *Neural Networks in Pattern Recognition*, Oxford: OUP.

Brown, M. and Harris, C., (1994), *Neurofuzzy Adaptive Modelling and Control*, New York: Prentice Hall.

Clinch, M.R., Harris, S.J., Hepples, W., Holroyd, N.J.H., and Wood, J.V. (2000), *Mater. Sci. Forum*, **331-337**, 861.

Christensen, S.W., Kandola, J.S., Femminella, O., Gunn, S.R., Reed, P.A.S. and Sinclair, I., (2000), *Mater. Sci. Forum*, **331-337**, 533.

Holroyd, N.J.H. and Hepples, W., (1999), U.S. Patent 5,932,037

Humphreys, F.J. and Hatherly, M., (1995), *Recrystallization and Related Annealing Phenomena,* Elsevier Science Ltd.

Woodward, A.R. and Bates, P.N., (1987), *Alum. Ind.* **6**, 17.